Journal of Materials Science & Technology 50 (2020) 103–114

Contents lists available at ScienceDirect

Journal of Materials Science & Technology

journal homepage: www.jmst.org

Research Article

Achieving a strong polypropylene/aluminum alloy friction spot joint via a surface laser processing pretreatment

S.C. Han[a,b], L.H. Wu[a,*], C.Y. Jiang[a], N. Li[a], C.L. Jia[a], P. Xue[a], H. Zhang[a], H.B. Zhao[a], D.R. Ni[a], B.L. Xiao[a,*], Z.Y. Ma[a]

[a] Shenyang National Laboratory for Materials Science, Institute of Metal Research, Chinese Academy of Sciences, Shenyang, 110016, China
[b] Department of Materials Science and Engineering, Guilin University of Technology, Guilin, 541006, China

ARTICLE INFO

Article history:
Received 28 November 2019
Received in revised form 19 January 2020
Accepted 17 February 2020
Available online 9 March 2020

Keywords:
Friction stir welding
Hybrid joint
Metal
Polymer
Surface treatment
Interface

ABSTRACT

Strong metal/non-polar plastic dissimilar joints are highly demanded for the lightweight design in many fields, which, however, are rather challenging to achieve directly via welding. In this study, we designed a laser processing pretreatment on the Al alloy to create a deep porous Al surface structure, which was successfully joined to the polypropylene (PP) via friction spot welding. A maximum joint strength of 29 MPa was achieved, the same as that of the base PP (i.e. the joint efficiency reached 100%), much larger than ever reported. The joining mechanism of the Al alloy and the PP was mainly attributed to the large mechanical interlocking effect between the laser processed Al porous structure and the re-solidified PP and the formation of chemical bond at the interface. The deep porous Al surface structure modified by laser processing largely changed the Al–PP reaction feature. The evidence of the C—O—Al chemical bond was first time found at the non-polar plastic/Al joint interface, which was the reaction result between the oxide on the Al alloy surface and thermal oxidization products of the PP during welding. This study provides a new way for enhancing metal-plastic joints via surface laser treatment techniques.

© 2020 Published by Elsevier Ltd on behalf of The editorial office of Journal of Materials Science & Technology.

1. Introduction

In recent years, with the increasing demand for lightweight in automobile, aerospace, electronics and other fields, plastics and their composites have been applied more and more widely in these fields due to their light weight, high specific strength, excellent insulation, corrosion resistance and good design freedom [1]. In order to combine both the advantages of plastics and metals, the joining of plastics to metals has been drawn a lot of attentions. However, due to the great difference in chemical, mechanical and thermal properties between metals and plastics, the joining between plastics and metals is rather challenging [2].

Adhesive bonding and mechanical fastening are traditional processes to join plastics and metals [3,4]. However, these joining technologies have their drawbacks. For the adhesion method, it is toxic, greatly affected by environmental factors, especially temperature, requires long processing time for effectively joining, and easily makes environmental pollution. Mechanical fastening usually introduces extra weight for the components, produces stress concentration near the hole and limits the flexibility of the workpiece design. In order to avoid the problems above, new welding processes, such as ultrasonic welding [5,6], laser welding [7,8] and friction stir welding (FSW) [9,10] become a new choice for the joining of metals and plastics. Balle and Eifler [11] realized the joining between AA5754 Al alloy and carbon fiber reinforced polyamide 66 (CF-PA66) through ultrasonic welding, and the joint strength was 32.5 MPa. Katayama and Kawahito [8] achieved the joining between Zn-coated steel and PA6 through laser welding, and the joint strength reached 3.3 kN. Subsequently, Jung et al. [12] also conducted laser welding on the 5052 Al alloy and the PA6, and the joint strength also reached 3.0 kN. It indicates that both the laser welding and ultrasonic welding are feasible for joining metals to plastics and their composites. However, these two welding techniques have their shortcomings. For example, laser welding is generally involved with a plastic degradation, and thus produces large quantities of bubbles, which largely affects the joint quality and strength [8,12]. Also, the cost of the laser equipment itself and the consumables is high. Besides, the welding effect for some metals with poor laser absorption such as copper and opaque plastic

* Corresponding author.
E-mail addresses: lhwu@imr.ac.cn (L.H. Wu), blxiao@imr.ac.cn (B.L. Xiao).

https://doi.org/10.1016/j.jmst.2020.02.035
1005-0302/© 2020 Published by Elsevier Ltd on behalf of The editorial office of Journal of Materials Science & Technology.

is not ideal. For ultrasonic welding, only spot welding experiments can be carried out and the size of joined materials is limited.

To avoid these disadvantages above, FSW, a solid-state welding technique, which has been widely studied in Al, Mg, Ti, steel etc. [13–17], seems also a good selection for the joining of metals and plastics [18]. The principle of FSW for lap joining of metals and plastics is as follows. During FSW of the metal and the plastic, heat is generated by the friction between the rotated shoulder and the metal, which is transferred to the plastic under the metal to melt the plastic. The melted plastic is then pushed to the metal under the shoulder to realize the joining of the metal and the plastic [19,20].

Compared with laser welding and ultrasonic welding, FSW mainly shows several advantages when welding metals and plastics as follows. First, the size of the welded component is not limited. Second, the heat input can be controlled to a low extent, which is beneficial to avoiding resin degradation. Third, it is not subjected to the optical properties of materials such as light transmission. Fourth, the thermal-mechanical process can be regulated to control the joint bonding, and the welding pressure is benefit for squeezing the bubble out of the joint. Therefore, FSW shows great advantages in the metal/plastic joining.

Recently, many researchers have reported the FSW of metals to plastic based materials [19–24]. Eslami et al. [21] had highly summarized the significance of FSW for the joining of plastics and metals. Liu et al. [20] successfully realized the joining of 6061 Al alloy and polyamide 6 (PA6) by friction lap welding (FLW). Huang et al. [22] achieved the joining between the 6061 Al alloy and polyether-ether-ketone (PEEK) through friction stir lap welding, and the joint strength reached 20 MPa. Nagatsuka et al. [9] pointed out that the PA6 based carbon fiber reinforced plastic (CFRP) is effectively bonded to the 5052 Al alloy by FLW, possibly because a hydrogen bond was formed at the interface as the reaction result of the polar functional group (amide group, CONH) of PA6 with MgO on the Al alloy surface. For such plastics containing polar functional groups (e.g. PA6, PEEK), Liu et al. [25] believed that their main joining mechanism with metals was associated with the formation of chemical bond, which was the reaction result between the functional group (e.g. carbonyl group) of the plastics and the oxide of the metal surface during the welding process [26]. Therefore, the successful joining between metals and plastics with functional group should be mainly related to the chemical or hydrogen bond formed by the functional group of the plastics and the oxide of metals during FSW.

For the non-polar plastics without polar function group, however, it was very difficult to form chemical or hydrogen bonds at the interface during FSW. Therefore, it might to be much more difficult to achieve a strong joint by FSW [27–29]. For example, Shahmiri et al. [28] successfully achieved the joining between the 5052 Al alloy and the PP by friction stir spot (lap) welding (FSLW) via increasing stirring effect to increase mechanical interlocking, but the joint strength was just about 5.1 MPa. Pabandi et al. [27] achieved the joining of the 5052 Al alloy and the carbon fiber reinforced polypropylene (CF-PP) by a new refilled FSLW, but the tensile shear force (TSF) of the joint was just 0.35 kN. Nagatsuka et al. [29] found that the polyethylene (PE) without surface treatment could not be joined to the carbon steel, and the PE after a corona discharge treatment could be joined to the carbon steel, since the polar functional group was formed on the PE surface, but the joint strength was still only about 4.2 MPa.

Therefore, it is rather difficult to realize the joining of metals and non-polar plastics without functional groups. Or even if successfully joining, such joints have a low strength. Actually, non-polar plastics such as PP and PE are very commonly used in the practical engineering application, and strong joints of metals and non-polar plastics are highly demanded in the practical application. However, the difficulty to achieve strong joints between metals and non-polar plastics has become the main reason for limiting their engineering applications. Therefore, to enhance the strength of the joint of metals to plastics without functional group has been an imminent thing. It has been reported that the surface structure and state of the welded metals largely affected the joint strength [9,29]. Therefore, in this work, the welded Al alloy surface was modified by a laser processing pretreatment, and was then joined to PP by FSLW. The object is (i) to explore the feasibility of achieving a strong joint of metals to non-polar plastics via an assistant surface laser pretreatment technique, and (ii) to clarify the joining mechanism between the laser pretreated metals and non-polar plastics.

2. Materials and methods

The as-received materials were the injection molding PP (PP, 200 mm × 80 mm × 2.8 mm) plate and 5182 Al alloy (240 mm × 120 mm × 1.2 mm) plate. The nominal chemical compositions of the 5182 Al alloy were as follows: Mg (4.89%), Mn (0.45%), Fe (0.2%), Si (0.1%), Zn (< 0.01%), Cu (< 0.01%). During the experiment, in order to avoid severely breaking the Al alloy microstructure, a pulse laser with a small power of 100 W was used to process the Al alloy surface, and the laser processing parameter was: pulse frequency, 100 kHz, scan speed, 7000 mm/min, and hatch distance (between two consecutive lines) 0.4 mm. Since the laser power was very small, and only small grooves with a small depth on the Al surface were made after each scanning. In order to explore the influence of the groove depth and structure on the joining quality and mechanical property of the joints, the number of laser scanning was set as the variable of the welding experiment in this study, which were 1, 5, 10, 20 and 40 times for each path with a cross-vertical scanning.

Before welding, the 5182 Al alloy and PP were polished with 800# silicon carbide sandpaper, rinsed with alcohol, and finally blown dry with a blower. The welding tools consisting of a flat shoulder 15 mm in diameter with and without a pin was used for FSLW. For the welding tool with a pin, the tool of the shoulder with 15 mm in diameter, the tapered pin with screw thread 5 mm in root diameter and 1.7 mm in length was used. During welding, the temperature of the contact surface between the metal and the plastic was measured with a k-type thermocouple. The different FSLW parameters were explored for the joining of laser processed Al alloys and PP using a welding tool without a pin, and the parameter range was: rotation rates of 1000−2000 rpm with an internal of 500 rpm, plunge depths of 0.3–0.5 mm with an internal of 0.1 mm, and dwell time of 3−6 s with an internal of 1 s. By observing the joint morphologies, the optimization welding parameter was determined as follows: rotation rate 1500 rpm, plunge depth 0.5 mm and dwell time 6 s.

The lap area of the 5182 Al alloy and the PP was 30 mm × 30 mm during the FSLW experiment. After the spot welding test, the joint was subjected to tensile shear tests using a Shimadzu UH-F100OKNC hydraulic universal testing machine at the crosshead speed of 1 mm/min. Three samples were welded for each parameter for stretching to reduce errors. The profilometer with laser scanning confocal microscope (LSM 700) was used to measure the metal surface roughness. Optical microscopy (OM, Axio Observer Z1) and scanning electron microscopy (SEM, FEI Quanta 600) with energy dispersive X-ray spectroscopy (EDS, Oxford) were used to observe the macroscopic morphology of joints. In addition, the samples were characterized by X-ray photoelectron spectroscopy (XPS) and Fourier transform infrared spectroscopy (FT-IR). XPS analyses of the samples were conducted using an ESCALAB 250 photoelectron spectrometer with an Al-anode at a total power dissipation of 150 W. A Nicolet iN10MX&iS10 FT-IR system in the reflection mode was used for FT-IR analysis. A minimum of 3600 scans was employed for each spectrum and the resolution was 2 cm^{-1}.

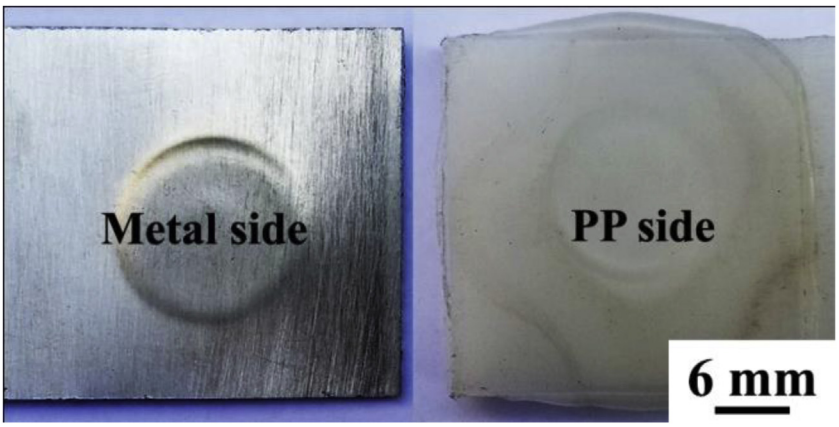

Fig. 1. Typical surface morphologies with separation directly after friction stir spot welding of 5182 Al alloy and PP using a tool without a pin.

3. Results and discussion

3.1. Direct joining of the Al alloy and the PP via friction stir spot welding

In this study, we first explored the direct joining of the 5182 Al alloy to the PP by friction stir spot welding using the welding tool with and without a pin at different parameters. The experimental results showed that the metal and the PP were directly separated, or separated during the following cutting. It suggested that the effective joining could not be achieved between the Al alloy and PP by the direct friction stir spot welding, and the typical joint surface morphology is shown in Fig. 1. It was obvious that there was a rather large difficulty to successfully weld metals with PP-like non-polar plastics, as was mentioned in the **Introduction** section. As we know, the joining mechanism between metals and plastics might be associated with chemical bond, hydrogen bond, or mechanical interlocking [8]. It is very difficult to form a chemical bond or hydrogen bond at the metal–PP interface. But it has been reported that a successful joining of the Al alloy to the PP and its composite was achieved by friction stir lap welding mainly by increasing the mechanical interlocking effect, although the joint strength was still very small [27,28]. Therefore, to further largely increase the joint strength, increasing the mechanical interlocking effect by modifying the surface structure might be a very important way to enhance the strength of metal-plastic joints [9,23].

3.2. Feasibility of friction spot joining of the PP and the Al alloy via laser processing pretreatment

As we know, there are some methods to pre-treat the metal surface, such as grinding with sandpaper, sandblasting, surface anodizing, surface laser processing etc. In these surface pretreatment methods, the laser processing method could well control the metal surface structure including the distance, depth, size and roughness of the laser processed pores in a large range. Therefore, the laser processing method was selected to pre-treat the Al alloy surface in this study. The surface of the Al alloy was laser processing pretreated by using a pulsed laser source, and in order to obtain different surface structures, the metal surface was treated via the laser pulse by different scanning number. The schematic of the laser processing is shown in Fig. 2(a), and the typical modified surface structures by the laser processing pretreatment are shown in Fig. 2(b–e). It was obvious that the morphology of the metal surface changed significantly after the laser processing (Fig. 2(b and c)). By observing the cross section and the topographical view of the metal surface after the laser pretreatment (Fig. 2(d and e)), one can find that after the laser processing pretreatment, the flat surface has changed into a deep porous surface.

In order to more accurately describe the effect of the laser scanning number on the depth of the groove of the metal surface, the depth of the 100 continuous grooves on the Al alloy for different laser scanning number was measured. In addition, the roughness was also measured, as shown in Fig. 3. It was obvious that as scanning number increased, the depth and roughness of the groove gradually increased. For example, the average groove depth and the roughness were only 4.60 μm and 1.92 μm for the laser scanning of 1 time, which increased into 59.6 μm and 13.76 μm when the laser scanning number was 10, increasing to even 205.42 μm and 45.76 μm, respectively for the scanning number of 40.

For these laser pretreated Al alloys with different surface structures, they showed a totally different welding feature with the PP, and the welding and the tensile results are shown in Fig. 4. For most of the Al alloys by the laser pretreatment, the effective joint with the PP was successfully achieved expect for that only scanning 1 time, and the typical joint is shown in Fig. 4(a). From Fig. 4(b), it was obvious when the number of laser scans was 1, the joint strength was 0, and the Al alloy and the PP were directly separated apart after welding. As was mentioned above, the PP itself does not have polar functional groups, it was difficult to form chemical or hydrogen bond, and the mechanical interlock between the metal and the plastic after welding was an important joining mechanism. However, the average depth of the grooves was only 4.6 μm for laser scanning 1 time, and thus there was no effective mechanical interlock effect after welding. As the laser scanning number increased, the TSF increased, and when the laser scanning time reached 10, the TSF of the joints almost remained unchanged. For scanning 5 times, the joint fractured along the Al–PP interface with a normal tensile shear strength (TSS) of about 11 MPa, but when the scanning time increased over 10, the joints all fractured at the PP base material. The maximum TSF of the joint reached 2.4 kN, and the corresponding normal TSS of was about 29 MPa, the same as that of the PP. It means that the welding efficiency was reached 100% in this study.

In order to compare to the joint strength in the literatures reported, the maximum normal TSS and TSF of hybrid lap joints of metals to non-polar polymers without any functional group for different welding techniques are summarized in Fig. 5 (the detailed explanation on the data and the assistant processing methods please refer to Appendix Table A1 and its text). Unlike many studies with only TSS for comparison, here we summarized both TSS and TSF of the non-polar plastic-metal hybrid joint, just because of the fact as follows. For lap welding in practical engineering application, the load is even more worthy of being noted than the strength, since some joints with a high strength but with a very small joining area,

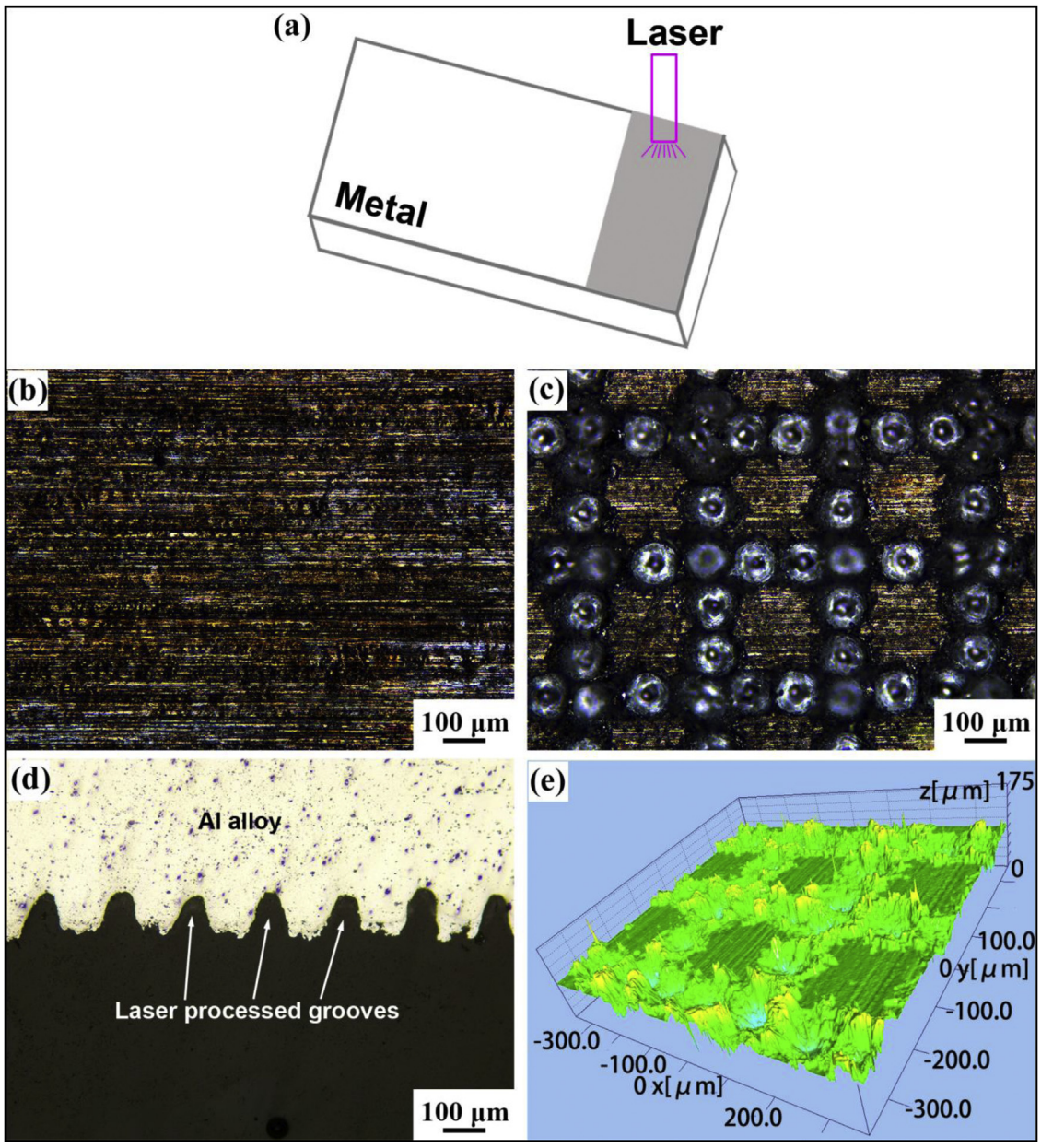

Fig. 2. (a) Schematic of laser processing pretreatment on Al alloy surface, and metallographic photos of Al alloy surface, (b) before pretreatment, (c) after laser processing pretreatment, (d) cross section after pretreatment, (e) topographical view of Al alloy surface measured by surface profilometer.

i.e. with a small TSF, still have small bearing capacity so that they might be limited for the engineering application. But TSF is largely affected by the tensile specimen width, and a used wider tensile specimen leads to a large TSF, even if with the same joint strength. Thus, in some cases, only the TSF could not be well compared for the joint bearing capacity. Therefore, It is more beneficial to comparing the joint bearing capacity when both the joint TSS and TSF. From Fig. 5, it was obviously found that both the maximum TSS and TSF were much larger than those ever reported [19,27–32], which suggested that the joint in this study had a good bearing capacity. Therefore, the laser processing surface pretreatment on the Al alloy combining with FSW is a good way to largely enhance the metal-plastic joint strength.

Temperature measurement experiments were carried out on the friction spot welding process of the Al alloy and PP, as shown in Fig. 6. The temperature at different interface position was measured, as shown in Fig. 6(a). The position 1″, position 2″ and position

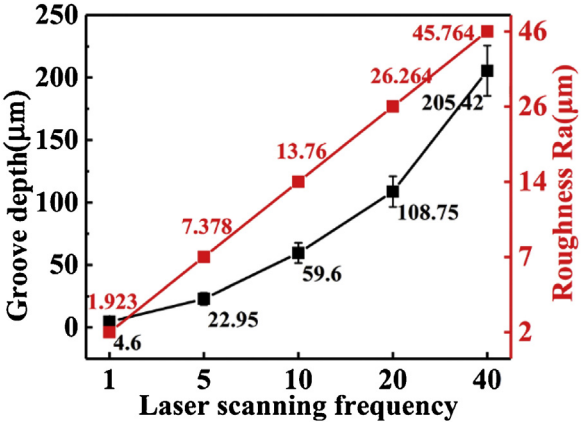

Fig. 3. Groove depth and roughness of Al alloy surface after laser processing for different scanning number.

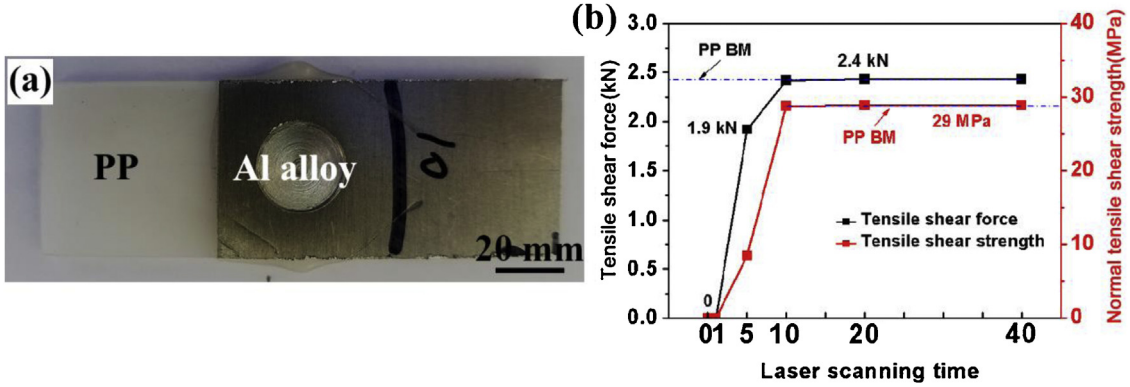

Fig. 4. (a) Typical macro surface image of friction spot joint of PP to Al alloy after laser processing pretreatment, (b) variation of tensile shear force and strength of joints with laser scanning number.

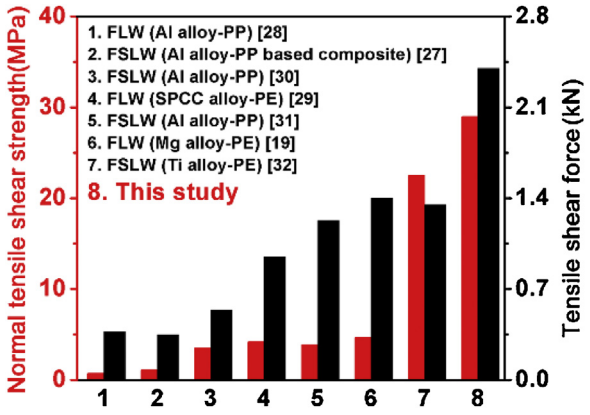

Fig. 5. Maximum normal tensile shear strength and force of non-polar plastic-metal hybrid joints from different researches. FLW and FSLW represent friction (stir) lap welding and friction (stir) spot lap welding, respectively. The red and black columns represent normal tensile shear strength and force, respectively in this figure.

3″ recorded the temperature of the positions away from the joint center point of 0 mm, 3.75 mm and 7.5 mm, i.e. the joint center, the center of the welding tool and the edge of the welding tool. The temperature measurement results are shown in Fig. 6(b). The welding temperature at the joint center was over the thermal decomposition temperature of the PP, but as the distance deviated from the center, the welding temperature was below the thermal decomposition temperature of the PP at the center and the edge of the welding tool. As we know, the temperature rising of the welded materials during FSLW mainly resulted from the friction heat between the welding tool and the welded materials, and the tool center could be regarded as a heat source to conduct heat around. During FSLW, the heat mainly generated at the top surface was conducted to the materials below. More heat but less hear dissipation was got in position 1 (interface center) than positions 2 and 3, since the materials in positions 2 and 3 were more far away from the heat source and were around by colder materials. Therefore, position 1 (the interface center) exhibited a higher peak temperature than positions 2 and 3 (deviated from the interface center).

In addition, the macrostructural cross sections of the welded joints of the laser scanning number of 5, 10, 20, and 40 were also observed, as shown in Fig. 6(c–f). It was found that a successful joining between the Al alloy and PP was achieved for the laser scanning number of 5-40. Also, mechanical anchors have formed at the interface since the plastic was pushed into the pores or grooves of the laser processed Al alloy. Besides, the mechanical anchoring effect increased when the laser processing time increased, since the laser processed groove depth increased. Therefore, the large mechanical interlocking effect should be an important reason for the large joint strength in this study.

The typical magnified image in Fig. 6(g) shows that no bubbles were observed in the joints. As we know, during the welding process of metals and plastics, thermal decomposition of the plastic was generally involved. After thermal decomposition of the plastic, a large amount of gas was often generated, such as water vapor, CO_2, CO, NO and NO_2, which remained in the joint to form bubbles [8,26]. The remaining bubbles in the joint may act as a pass path for the crack, reducing the joint strength [10,24]. However, in this study, no bubbles were observed at the joint maybe because of two aspects. On one hand, the decomposition temperature of the PP is 370 °C, as shown in Fig. 6(b), and only the temperature of ṗosition 1ïs slightly higher than this temperature, which means that there was a low extent of thermal decomposition during the welding process. On the other hand, crisscrossed grooves were formed on the metal surface after the laser surface treatment, and the original air in the groove and the gas generated by the thermal decomposition of the PP can be smoothly expelled out of the groove during the downward pressing of the shoulder. Both of the reason above made a joint without bubbles, which might be also a reason for the strong joint in this study.

3.3. *Microstructure of the Al–PP joint interface for different laser processed structures*

The SEM images of the joint interfaces corresponding to the positions for the thermocouple temperature measurement for laser scanning 5 times are shown in Fig. 7. At the center position of the joint, a good joining seemed to be made (Fig. 7(a)), but higher magnification shows that cracks or gaps existed between the Al alloy and the PP in most part of the interface (Fig. 7(b and c)). A detailed observation showed that a tight joining was successfully achieved at some part of the bottom of the grooves (Fig. 7(d)) although a number of cracks or gaps (the widest width was about 2.6 μm) were found in the grooves (Fig. 7(c)). It suggested that at the majority of the joint in the center, the joint was not tight bonded, but at some small part of positions, an effective tight joining was achieved.

At the center of the welding tool, i.e. about 3.75 mm away from the joint center (position 2 in Fig. 6(a)), a tight bonding was achieved at the bottom of the trench in the grooves, although a gap occurred at the corner of the trench, as shown in Fig. 7(e). At the edge of the welding tool, i.e. about 7.5 mm away from the joint center (position 3 in Fig. 6(a)), a tight bonding with no gap was observed at the joint interface of the Al alloy and the PP, as shown in Fig. 7(f). Therefore, the effective tight joining increased as the distance away from the joint center increased.

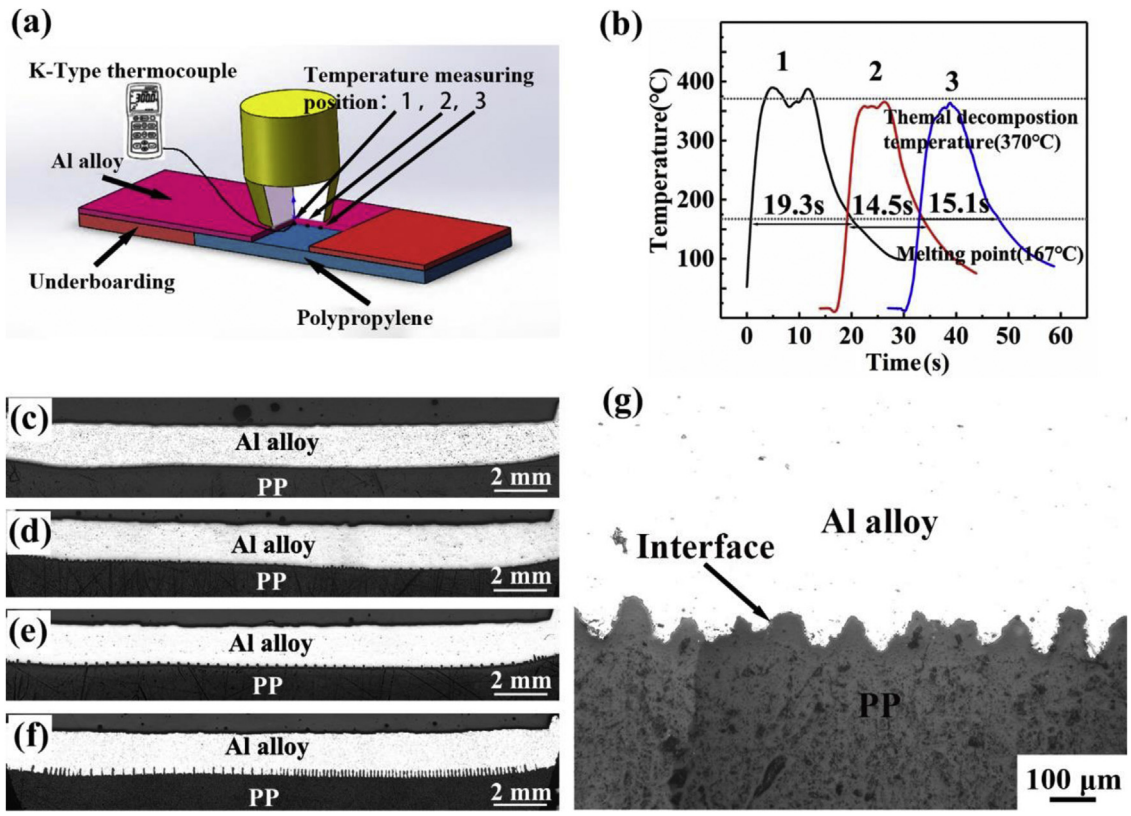

Fig. 6. (a) Temperature measurement position, (b) temperature measurement results, (c-f) cross sections of Al–PP joints with laser scanning number of 5, 10, 20 and 40, (g) typical microstructure of Al–PP joint for laser scanning 10 times.

As we know, during friction spot welding, the enough heat was conducted to the PP, resulting in the melting of the PP. The welding temperature was generally highest in the joint center, and thus the PP at the center first melted, which was extruded to the edge of the joint or to the laser processed grooves of Al alloys under the downward pressure of the shoulder. That means that the PP at the edge of the joint might be the first melted PP flown in, which even experienced a longer time of melting than that remained at the center. A longer contacting time between the melting PP and the Al alloy might make it easier to form a tight bonding at the edge of the joint than the center. In addition, the temperature at the joint center was greater than the decomposition temperature of the PP (Fig. 6(b)), whereby the PP might decompose to generate gases. These gases might also affect the interface bonding, although they were finally expelled out of the joint. When close to the edge of the welding tool, the temperature was below the thermal decomposition point, and no gas was formed at these positions, which would not affect the joining of the Al alloy and the PP.

As was shown above (Fig. 4), when the laser scanning number was over 10, the joint strength reached the maximum of 29 MPa. In order to explain the joining mechanism, the joint interfaces for 10–40 times were also observed in details and the typical SEM images of the joint interface for 10 and 40 times are shown in Fig. 8. For all the joints with different scanning number, the laser processed grooves were all fully filled with the PP. The mechanical interlock effect increased with increasing the laser scanning number (Figs. 7(a), 8 (a and b)).

In addition, as the laser scanning number increased, the extent of the tight joining increased. For 10 times, a tight bonding was only achieved at some positions of the interface, while at most of the joint interface, there was not a tight bonding, similar to that with 5 times. But for 40 times, at the majority of the joint interface, a tight bonding was achieved, as shown in Fig. 8(c). A higher magnification in Fig. 8(d) shows that the Al alloy and the PP have tightly bonded even at the nano scale, which might be the result that the chemical bond was achieved between the Al alloy and the PP, which will be discussed in the following section. As shown in Fig. 6(b), the welding temperature during friction spot welding was much higher than the melting temperature of the PP, and the time above the melting temperature exceeds 14 s. It means that an enough heat was probably provided to effectively join the PP and the Al alloy.

In order to further clarify the joint fracture behavior, the fracture surface morphology of the joint for 5 times was observed, as shown in Fig. 9. It was obvious that the joint was pulled apart along the Al–PP interface (Fig. 9(a)). Some residue was found on the fracture Al surface, and the residue was only present within the range of the shoulder diameter (15 mm). The magnification of the residue on the fracture metal surface is shown in Fig. 9(b). The Al and C elements were selected as the trace elements of the Al alloy and the PP, as shown in Fig. 9(c and d.) It was found that the grey material should be the Al alloy, and the black and white ones were the PP. From the fracture surface, it was found that the re-solidified PP inside the groove was directly pulled out of the metal grooves and only a small fraction of PP residue (the area ratio of 12.4%) was found on the fracture metal surface of the joint. It also suggested that only a small part of the interface in the joint had achieved a tight bond, agreeing well with the cross-sectional observation in Fig. 7.

Besides 5 times, the joint surface morphologies and interfaces after fracturing for over 10 times were also observed, and the typical images are shown in Fig. 10. When the laser scanning number was over 10, all the joints fractured at the PP base material (Fig. 10(a)). For 10 times, at most part of the joint interface, cracks with a big width appeared between the Al alloy and the PP after stretching, as shown in Fig. 10(b). Also, in some position, a tight bonding was still unchanged after stretching (Fig. 10(c)). Compared to the joint interface for 10 times before stretching (Figs. 6(g), 8 (a) and 10 (b)),

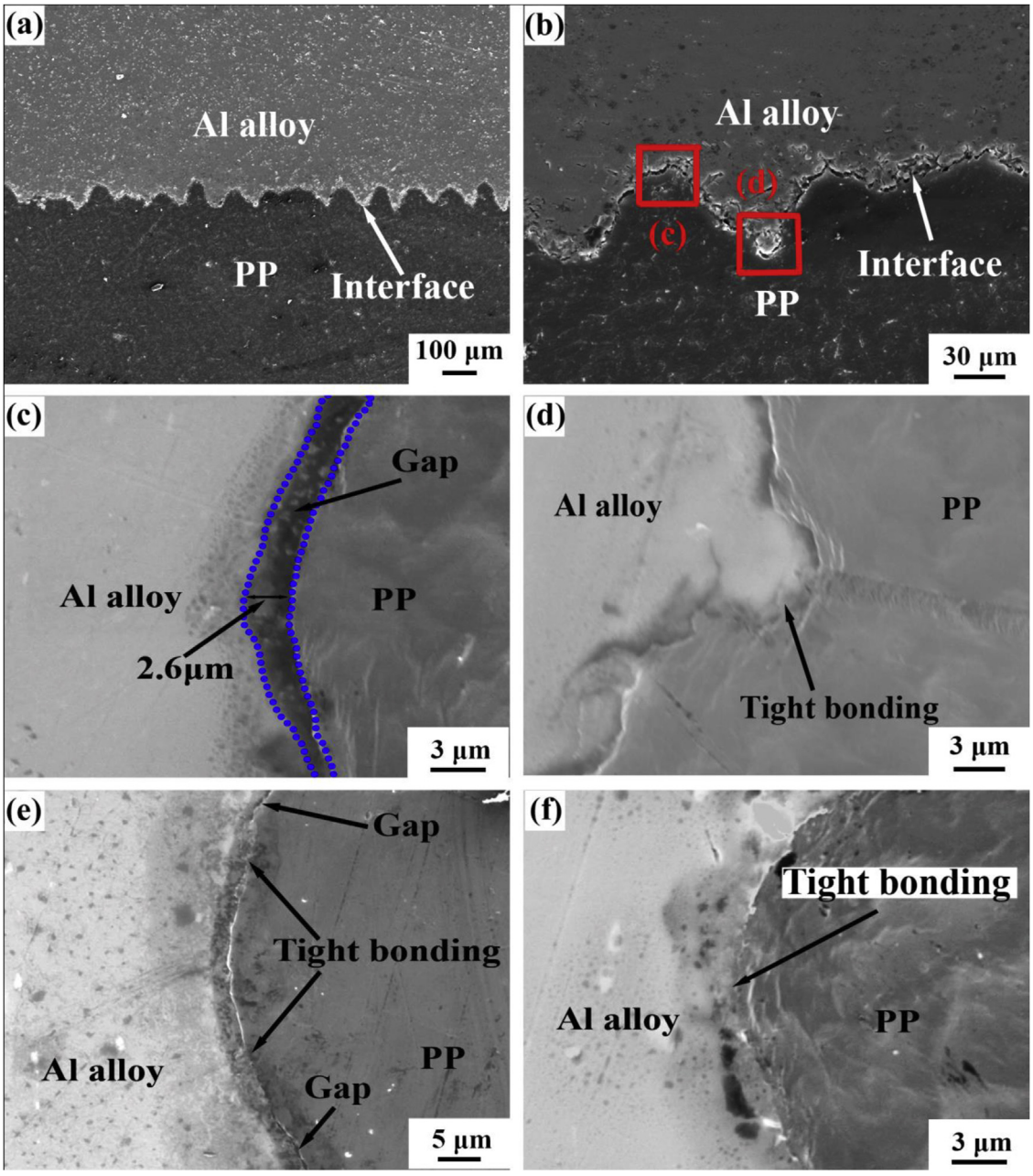

Fig. 7. SEM images of Al–PP joint for laser scanning 5 times: (a, b) interface at joint center (p̈osition 1ïn Fig. 6(a)), (c, d) high magnification of red frame in (b), (e, f) high magnified images of groove bottom at joint position of 3.75 mm away from joint center (p̈osition 2ïn Fig. 6(a)) and at joint position of 7.5 mm away from joint center (p̈osition 3ïn Fig. 6(a)).

it was obvious that the cracks at the interface became wider during the stretching process, although the total interface morphology did not change before and after stretching. Because there was not a tight bond in the most part of the joint interface, these positions were easily stretched apart. But for the positions with a tight bond, even if the joint was stretched to fracture, the tight bonding morphology remained unchanged (Fig. 10(c)). It suggested that there must be a large bond force for this tight joining.

For the joint with laser pretreated 40 times (the depth of the groove reached 234.7 μm), however, in the most part of the joint interface, the tight bonding state remained unchanged after tension, as shown in Fig. 10(d and f). It also indicated that a strong bond force must exist at the interface so that the tight bonding could not be stretched apart between the Al alloy and the PP even if there was a large load. Therefore, it could be speculated that a strong chemical bond might be formed between the Al alloy and the PP. In addition, in some interface positions, the Al anchors were even pulled to fracture (Fig. 10(e)), although the Al–PP interface was still tight bonded (Fig. 10(f)). The reason might be that the Al alloys experienced a large grain growth because of the large heat affecting during laser processing for too many times, resulting in the surface Al bead strength to drop, which thus reduced the mechanical interlocking force between the PP and the laser processed Al alloy.

3.4. Joining mechanism between the laser processed Al alloy and the PP

In order to verify the bonding mechanism, the as-received PP and the residue on the fracture metal surface were observed by

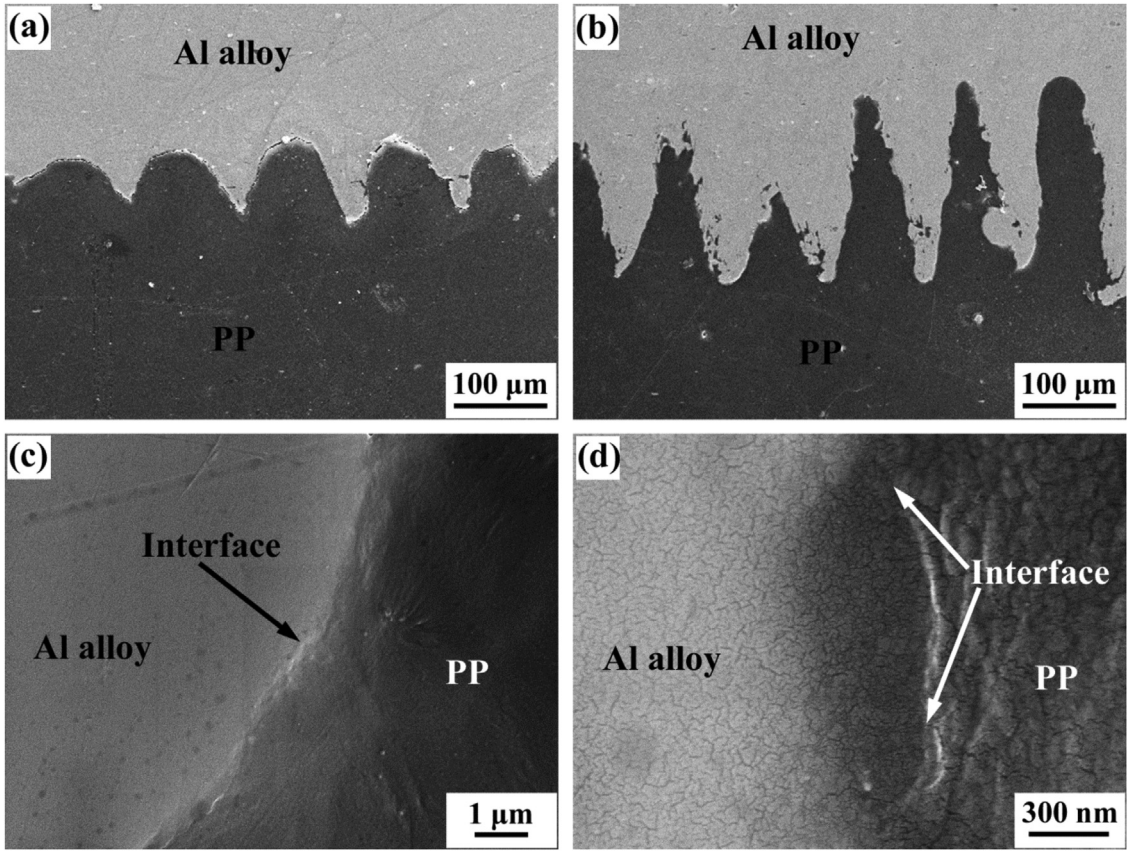

Fig. 8. SEM images of Al–PP interface of joints: (a) laser processing for 10 times, (b) laser processing for 40 times, (c, d) high magnification of Al–PP interface for 40 times.

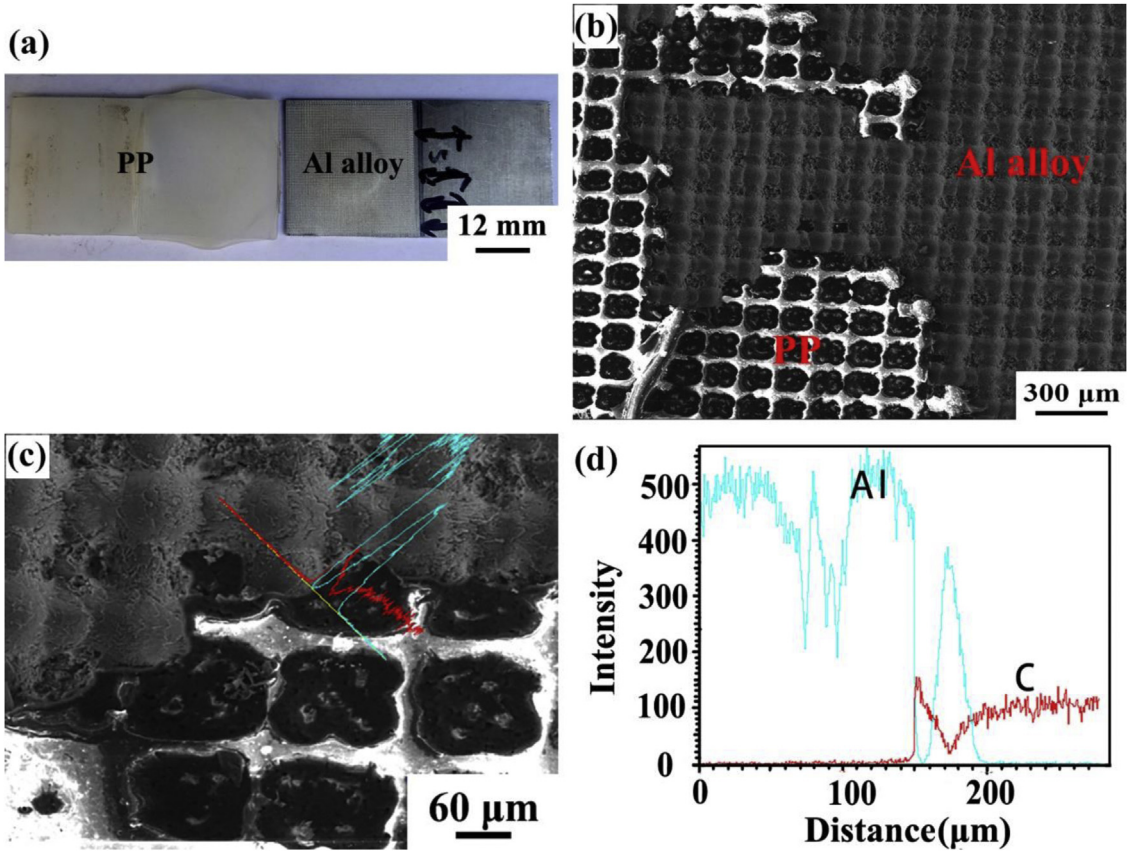

Fig. 9. (a) Joint surface morphology after stretching at laser scanning 5 times, (b) PP remained on metal side, (c, d) residual PP on metal side by SEM-EDS analysis.

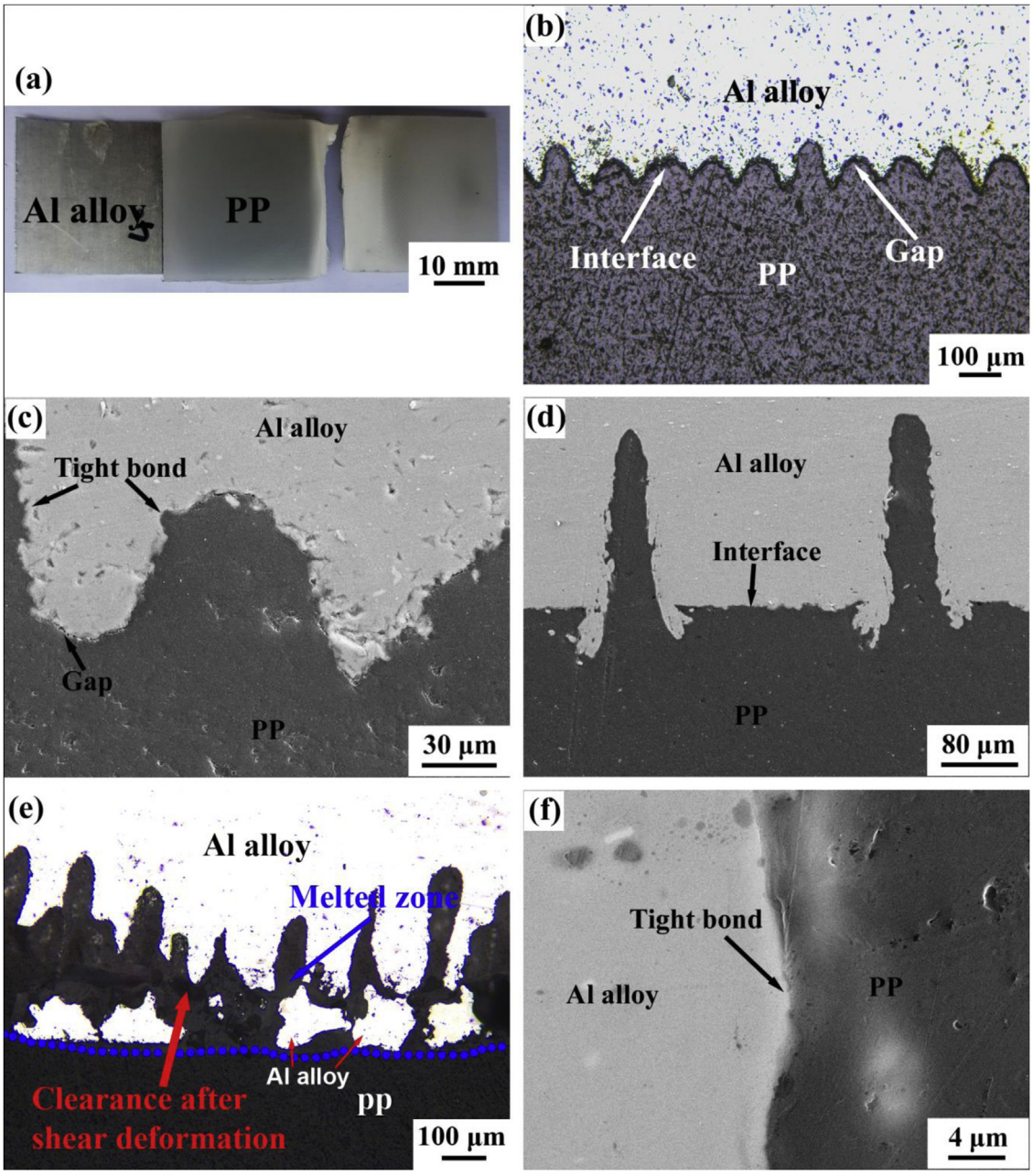

Fig. 10. (a) Typical fractured surface morphology of Al–PP joint for laser scanning 40 times after fracturing, (b) cross section of Al–PP joint for 10 times after fracturing, (c) high magnified SEM image of joint interface between Al alloy and PP for 10 times after fracturing, (d) most joint interface between Al alloy and PP for 40 times after fracturing, (e) Al anchors was pulled to fracture in some position of Al–PP joint for 40 times, (f) tight bonding at joint interface between Al alloy and PP for 40 times after fracturing.

FT-IR spectrum, as shown in Fig. 11. Comparing Fig. 11(a) with (b), it was found that a new spectral band appeared at the position of about 1650 cm^{-1} on the remaining PP on the fracture metal surface. As we know, a thermal oxidation process of the PP might occur at elevated temperature. In the process of thermal oxidation of the PP, it was reported that there was a carbonyl group (C═O bond) near the wavenumber of about 1715 cm^{-1} [33], but the wavenumber position of the C═O bond was also affected by hydrogen bond or some other chemical bond, absorbed to the low wavenumber position [7,33,34]. In this study, during the welding process of the metal and the plastic, it was generally believed that there was a chemical or hydrogen bond at the joint interface, which will be confirmed by the subsequent experiment result in this study. Thus, the stretching vibration of the C═O bond was probably affected by these bonds, and finally the wavenumber position of the C═O bond exhibited near about 1650 cm^{-1}.

In order to further determine the presence of the carbonyl group, XPS analyses of the PP and the residue on the fracture metal surface are shown in Fig. 12. A charging compensation was applied during data acquisition, and all the spectra were calibrated by setting the C1s hydrocarbon peaks to the positions of the binding energy of 285.0 eV. Fig. 12(a) shows that the PP base material only consisted of C—C and C—H bonds, and there were no other chemical bonds. The XPS analysis of the remaining PP on the fractured metal side showed that a carbonyl group (C═O bond) at the position of 287.1 eV as shown in Fig. 12(b), probably due to the thermal oxidation of the PP occurring during the spot welding process, which further confirmed the FT-IR results.

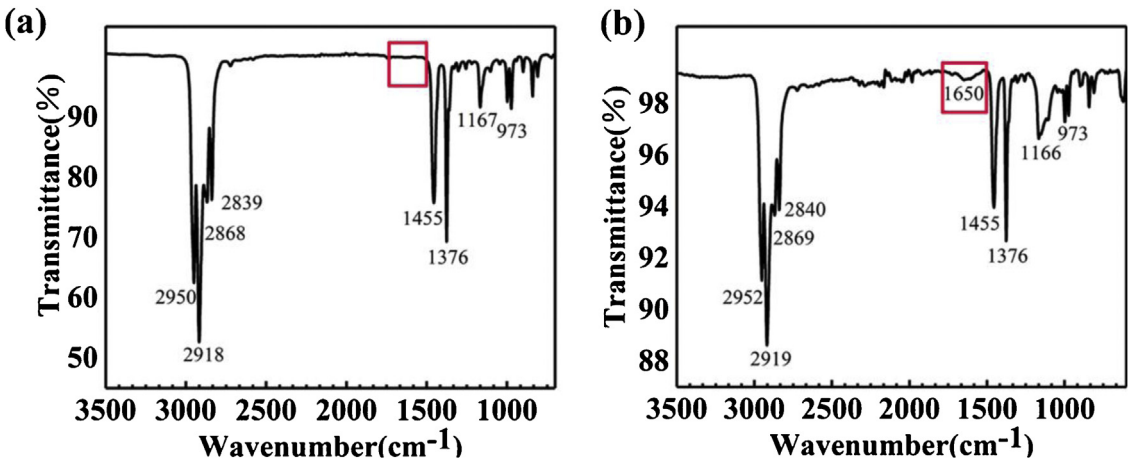

Fig. 11. FT-IR analysis of (a) as-received PP, (b) residue on metal side after joint fracture for laser scanning 5 times.

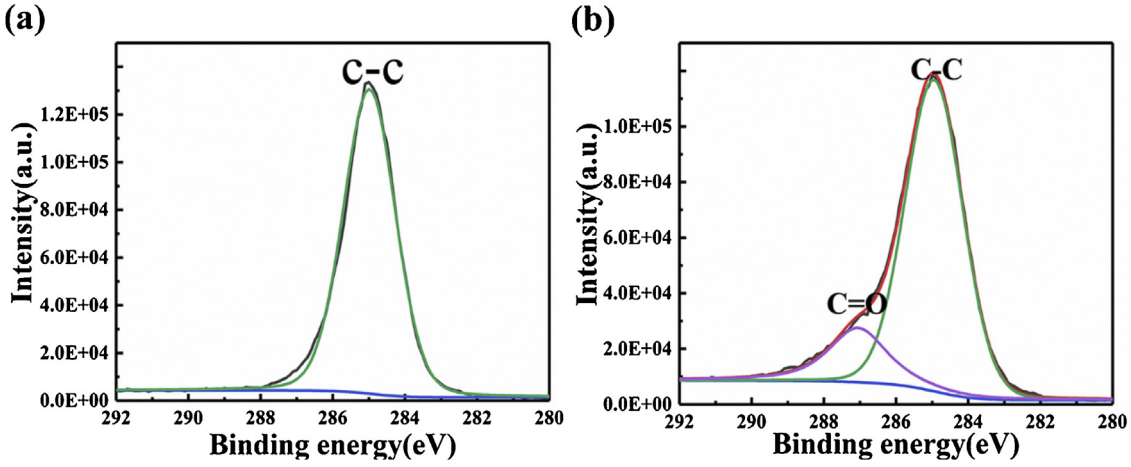

Fig. 12. XPS analysis of (a) as-received PP, (b) residue on metal side after joint fracture for laser scanning 5 times.

In order to further explain the joining mechanism of the Al alloy and the PP, the XPS analysis on the fractured Al alloy surface was carried out. As was mentioned above, after laser surface treatment, the metal surface is rather uneven (the roughness was even tens of micrometers) (Figs. 2 and 3). Therefore, it was rather difficult to detect the bonding type from the top surface since the detection area of the XPS was just several to dozen of nm from the top surface. Also, since the bonding layer at the Al–PP interface was only several to dozen nm or even less, which was much less than the XPS analysis spot of 0.5 mm × 1 mm. Thus, it seems impossible to detect the chemical bond from the cross section of the joint. As was mentioned in Fig. 1, after the test, the two parts of Al alloy and PP were directly separated with no PP on the metal side. While for the friction spot joints of Al alloy and glass fiber reinforced PP (GF-PP), two parts were also directly separated, but a small amount of PP stuck on the Al surface. Thus, in order to confirm the reaction products at the interface of the Al alloy and the PP, in this study, XPS analysis was performed on this fractured metal part of Al–GF-PP joints by direct friction spot welding, as shown in Fig. 13. The result shows that a new C—O—Al chemical bond was detected on the fracture metal surface. Compared to Fig. 12(b), this new C—O—Al chemical bond should be the reaction products between the PP and the Al alloys. As is well-known, PP only consists of C—C and C—H bonds, which is very difficult to bond with the Al alloys to form C—O—Al. But both the FI-IT and XPS results showed that a C=O bond was formed because of thermal oxidation of the PP. Therefore, the formation of C—O—Al bond should be the result of the reaction between C=O bond and the oxide on the Al surface. It also explains why the tight bond was found at the Al–PP interface (Figs. 7(f), 8 (c and d)). Therefore, the large strength of the laser processed Al–PP joint, the same as the PP base material, should be mainly attributed to the large mechanical anchors between the laser-processed porous Al with the extruded PP, and the C—O—Al chemical bond at the Al–PP interface.

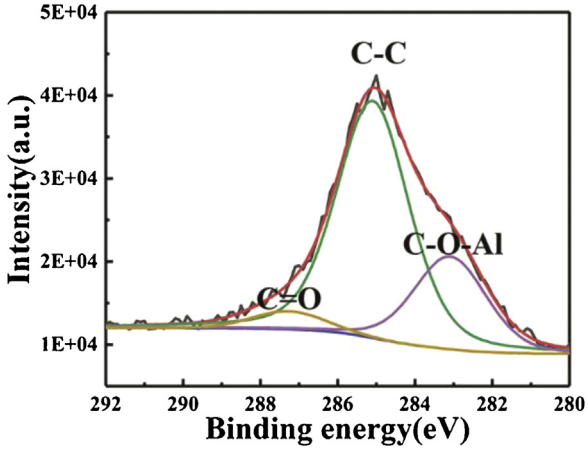

Fig. 13. XPS analysis of residue on Al alloy fracture surface of Al/glass fiber reinforced PP joint.

From the analysis and discussion above, a strong Al–PP joint was achieved after the laser process pretreatment. As the laser scanning number increased, the groove depth increased largely, and thus the mechanical anchoring effect between the laser-processed porous Al with the extruded PP increased, which was an important reason to increase the joint strength. Besides, with the laser processed depth increasing, the practical surface area of Al alloy for joining increased, which increased the chemical bonding area. Also, the increase of the laser processed depth could increase the chemical bonding extent. Thus, the effective joining between the laser processed Al alloy and the PP increased with the laser scanning number. But limited by the strength of the PP base material, the joint strength remained steady with that of the base PP. It should be pointed out that even if not limited by the base PP strength, the strength of Al–PP joint would not increase always with the scanning number. As was mentioned in Fig. 10(e), as the laser scanning number increased, the Al alloys experienced an increasing grain growth because of the large heat affecting during laser processing, which thus likely reduced the Al anchor strength. As a result, the Al anchors even started to fracture by the shear force (Fig. 10(e)). Therefore, an even higher scanning time was not beneficial to increasing the interface strength.

Besides, it should also be pointed out that it is generally regarded that PP is very difficult to react with metals, that is why it is so difficult to weld the PP and metals. However, in this study, an interesting phenomenon was found that as the Al surface was modified by the laser processing, the porous Al alloy could react with the thermal oxidation products of the PP, achieving a tight chemical bonding. For different surface structure, the reaction feature was different. It suggested that the modification of the metal surface could enhance the reaction feature between plastics and metals. It might be related to the different wetting, surface energy, roughness or other structure factors of materials, or/and the different temperature and stress distribution at different surface microstructures, which will be studied in our following work.

4. Conclusions

In this study, friction spot welding of the laser processed Al alloy and the PP was explored, and it was found that it was possible to make an effective joint between Al alloy and non-polar plastics. The conclusions are made as follows.

(1) An effective joining between the Al alloy and the PP can be achieved after the Al alloy surface was subjected to the laser pretreatment, although the Al alloy and the PP could not be successfully joined by direct friction stir spot welding.
(2) As the laser scanning number increased, the joint strength increased first, and then remained the maximum after 10 times. The maximum joint strength reached the same as that of the base PP of 29 MPa, and the joint efficiency reached 100%.
(3) The tight bonding was formed at the interface of the Al alloy and the PP, which was the result of the formation of Al—O—C chemical bond. The Al—O—C chemical bond was the reaction product of the oxide on the Al surface and the thermal oxidation product of the PP during welding.
(4) The strong strength of the Al–PP joint was mainly attributed to the large mechanical interlocking effect and the formation of the Al—O—C chemical bond. The mechanical interlocking effect and the chemical bonding area largely increased as the laser processed groove depth increased, resulting in an increased effective joining at the Al–PP interface with the laser processing number.

Acknowledgements

This work was supported by the National Natural Science Foundation of China (Nos. 51975553 and 51931009) and the IMR SYNL-T.S. Kê Research Fellowship.

Appendix A

Table A1
Maximum normal TSS and TSF of non-polar polymer-metal hybrid lap joints.

Method (materials)	Max TSF (kN)	Max normal TSS (% of plastic BM)	Normal joining area (mm^2)	Remark	Ref.
FLW (Al alloy-PP)	~0.37	~0.71* (2.8%)	20×25.8	Tool Φ20 mm; Interface fracture Reported max TSS: ~5.1MPa	[28]
FSLW (Al alloy-PP based composite)	0.35	~1.1* (~3.2%)	$\pi \times 10^2$	5052 Al alloy: Pre-threaded hole Φ4 mm; Tool Φ20 mm without pin; Interface fracture Reported max TSS: ~28 MPa	[27]
FSLW (Al alloy-PP)	0.54	~3.5* (~10%)	$\pi \times 7^2$	2219Al alloy: Pre-threaded hole Φ4 mm; Tool Φ14 mm without pin; Interface fracture	[30]
FLW(SPCC alloy-PE)	0.95	~4.2 (–)	15×15	PE: Corona-discharge; Tool Φ15 mm without pin; Interface fracture	[29]
FSLW (Al alloy-PP)	1.23	~3.9* (–)	$\pi \times 10^2$	5052 Al alloy: plasma electrolytic oxidation; Pre-drilled hole Φ5 mm; Tool Φ20 mm; Interface fracture	[31]
FLW (Mg alloy-PE)	~1.4	4.67 (–)	15×20	Low density PE: Corona-discharge; Mg alloy: plasma electrolytic oxidation; Tool Φ15 mm without pin; Interface fracture	[19]
FSLW (Ti alloy-PE)	~1.35	~22.5 (~64%)	$\pi \times 5^2$	Ti-6Al-4 V alloy: 3D printed, porous; Tool Φ10 mm without pin; PE fracture	[32]
FSLW (Al alloy-PP)	**2.4**	**29** (100%)	$\boldsymbol{\pi \times 7.5^2}$	5052 Al alloy: laser processing, porous; Tool Φ15 mm without pin; PP BM fracture	**This study**

* Some papers (e.g. [27,28] only used the tool pin area or hole area as the joining area for the metal-plastic friction (spot) lap joints, but strictly speaking, the materials under the whole tool area have great chance to be joined due to the temperature and pressure generated by the tool. Therefore, in this Table, in order to calculate the normal TSS for comparison, tool shoulder width × sample width and tool shoulder area were set as the normal joining area for lap welding and spot lap welding, respectively. TSS = TSF/normal joining area, when fracturing along the shear interface; TSS = TSF/(tensile specimen width × tensile specimen thickness), when fracturing at the plastic base material. It should be noted that the normal maximum TSS in this table from [27,28] was much lower than that reported just because the normal joining area for calculation was changed.

References

[1] B. Wielage, D. Richter, H. Mucha, T. Lampke, J. Mater. Sci. Technol. 24 (2008) 953–959.
[2] A. Pramanik, A.K. Basak, Y. Dong, P.K. Sarker, M.S. Uddin, G. Littlefair, A.R. Dixit, S. Chattopadhyaya, Compos. Part A 101 (2017) 1–29.
[3] J.M. Arenas, C. Alía, J.J. Narbón, R. Ocaña, C. González, Compos. Part B 44 (2017) 417–423.
[4] J.P. Kabche, V. Caccese, K.A. Berube, R. Bragg, Compos. Part B 38 (2007) 66–78.
[5] F. Balle, G. Wagner, D. Eifler, Adv. Eng. Mater. 11 (2009) 35–39.
[6] F. Balle, G. Wagner, D. Eifler, Materialwiss. Werkstofftech. 38 (2007) 934–938.
[7] X.H. Tan, J. Zhang, J.G. Shan, S.L. Yang, J.L. Ren, Compos. Part B 70 (2015) 35–43.
[8] S. Katayama, Y. Kawahito, Scr. Mater. 59 (2008) 1247–1250.
[9] K. Nagatsuka, S. Yoshida, A. Tsuchiya, K. Nakata, Compos. Part B 73 (2015) 82–88.
[10] L.H. Wu, K. Nagatsuka, K. Nakata, J. Mater, Sci. Technol. 34 (2018) 192–197.
[11] F. Balle, D. Eifler, Materialwiss. Werkstofftech. 43 (2012) 286–292.
[12] K.W. Jung, Y. Kawahito, M. Takahashi, S. Katayama, J. Laser Appl. 25 (2013) 032003.
[13] L.H. Wu, X.B. Hu, X.X. Zhang, Y.Z. Li, Z.Y. Ma, X.L. Ma, B.L. Xiao, Acta Mater. 166 (2019) 371–385.
[14] R. Nandan, T. DebRoy, H.K.D.H. Bhadeshia, Prog. Mater. Sci. 53 (2008) 980–1023.
[15] L.H. Wu, D. Wang, B.L. Xiao, Z.Y. Ma, Scr. Mater. 78–79 (2014) 17–20.
[16] L.H. Wu, H. Zhang, X.H. Zeng, P. Xue, B.L. Xiao, Z.Y. Ma, Sci. China Mater. 61 (2018) 417–423.
[17] F.C. Liu, Y. Hovanski, M.P. Miles, C.D. Sorensen, T.W. Nelson, J. Mater. Sci. Technol. 34 (2018) 39–57.
[18] Y.X. Huang, X.C. Meng, Y.M. Xie, J.C. Li, L. Wan, Compos. Part A 112 (2018) 328–336.
[19] F.C. Liu, J. Liao, Y. Gao, K. Nakata, Sci. Technol. Weld. Joining 20 (2015) 291–296.
[20] F.C. Liu, J. Liao, K. Nakata, Mater. Des. 54 (2014) 236–244.
[21] S. Eslami, P.J. Tavares, P.M.G.P. Moreira, Int. J. Adv. Manufact. Technol. 89 (2016) 1677–1690.
[22] Y. Huang, X. Meng, Y. Wang, Y. Xie, L. Zhou, J. Mater. Proc. Technol. 257 (2018) 148–154.
[23] S.M. Goushegir, J.F. dos Santos, S.T. Amancio-Filho, Mater. Des. 54 (2014) 196–206.
[24] L.H. Wu, K. Nagatsuka, K. Nakata, J. Mater. Sci. Technol. 34 (9) (2018) 1628–1637.
[25] F.C. Liu, P. Dong, W. Lu, K. Sun, Appl. Surf. Sci. 466 (2019) 202–209.
[26] Z. Zhang, J.-G. Shan, X.-H. Tan, J. Zhang, Int. J. Adhes. Adhes. 70 (2016) 142–151.
[27] H. Karami Pabandi, M. Movahedi, A.H. Kokabi, Compos. Struct. 174 (2017) 59–69.
[28] H. Shahmiri, M. Movahedi, A.H. Kokabi, Sci. Technol. Weld. Joining 22 (2) (2016) 120–126.
[29] K. Nagatsuka, D. Kitagawa, H. Yamaoka, K. Nakata, ISIJ Int. 56 (2016) 1226–1231.
[30] M. Paidara, O.O. Ojob, A. Moghanianc, H.K. Pabandid, M. Elsae, J. Mater. Process. Technol. 273 (2019) 116272.
[31] S. Aliasghari, M. Ghorbani, P. Skeldon, H. Karami, M. Movahedi, Surf. Coat. Technol. 313 (2017) 274–281.
[32] K. Chen, B. Chen, S. Zhang, M. Wang, L. Zhang, A. Shan, Mater. Des. 132 (2017) 178–187.
[33] S. Qian, T. Igarashi, K. Nitta, Polym. Bull. 67 (2011) 1661–1670.
[34] Y. Feng, L. Zhou, N. Dong, X. Hong, China Plast. 17 (2003) 87–90 (In Chinese).